A Schlenk flask was charged with 18 (0.197 g, 0.311 mmol), CH$_2$Cl$_2$ (ca. 10 mL), and a stir bar. The resulting orange solution was cooled to −78 °C, and HBF$_4$·O(C$_2$H$_5$)$_2$ (41.0 μL, 0.312 mmol) was added by syringe with stirring. The solution turned light orange, and after 10 min ether (ca. 15 mL) was added. A dark yellow powder precipitated (0.154 g, 0.214 mmol, 69%), and the flask was transferred to a glovebox. The powder was collected by filtration and dried in vacuo. A portion of the solid was dissolved in CD$_2$Cl$_2$. A ^{1}H NMR spectrum at −60 °C showed 19$^+$BF$_4^-$ of ca. 85% purity.[45]

Rate Measurements. The following experiment is representative. A 5-mm NMR tube was charged with 2 (0.013 g, 0.023 mmol) and CD$_2$Cl$_2$ (0.60 mL) in a glovebox and capped with a septum. The tube was placed in a −78 °C bath, and after 10 min,

HBF$_4$·O(C$_2$H$_5$)$_2$ (2.7 μL, 0.023 mmol) was added by syringe. The tube was shaken and placed in a −85 °C NMR probe. A ^{1}H NMR spectrum was recorded and showed formation of 1$^+$BF$_4^-$. The tube was returned to the −78 °C bath and precooled CH$_3$CN (11.9 μL, 0.230 mmol) was added by syringe. The tube was shaken and transferred to a −38.5 °C NMR probe. The disappearance of 1$^+$BF$_4^-$ and appearance of 3$^+$BF$_4^-$ was monitored through 85% completion by integration of the cyclopentadienyl ^{1}H NMR resonances. Identical rate constants were obtained from ln [1$^+$-BF$_4^-$] and ln (1 − [3$^+$BF$_4^-$]) vs time plots (k_{obsd} = (11.6 ± 1.0) × 10^{-4} s^{-1}).[37]

Synthesis, Structure, and Reactivity of Bridging Halide Complexes of the Formula [(η⁵-C₅H₅)Re(NO)(PPh₃)]₂X⁺BF₄⁻. Preferential Binding of One Enantiomer of Halide Complexes (η⁵-C₅H₅)Re(NO)(PPh₃)(X) by the Chiral Lewis Acid [(η⁵-C₅H₅)Re(NO)(PPh₃)]⁺

Charles H. Winter, Atta M. Arif, and J. A. Gladysz*

Department of Chemistry, University of Utah, Salt Lake City, Utah 84112

Received May 17, 1988

Reactions of halide complexes (η⁵-C₅H₅)Re(NO)(PPh₃)(X) (X = I, **7**; X = Br, **8**) and AgBF$_4$ in refluxing benzene gives bridging halide complexes (*RR,SS*)-[(η⁵-C₅H₅)Re(NO)(PPh₃)]₂X⁺BF₄⁻ exclusively as *dl* diastereomers (X = I, (*RR,SS*)-**4**, 59%; X = Br, (*RR,SS*)-**5**, 54%). Reaction of optically active (+)-(*R*)-**7** and dichloromethane complex (*S*)-[(η⁵-C₅H₅)Re(NO)(PPh₃)(ClCH₂Cl)]⁺BF$_4^-$ ((*S*)-**1**) gives a complex mixture of products, including species derived from −CH₂Cl transfer from (*S*)-**1** to (+)-(*R*)-**7**. In no case is evidence for a meso diastereomer of a bridging halide complex observed. The structure of solvate (*RR,SS*)-**4**·(CHCl₂CHCl₂)$_{0.7}$ is verified by X-ray crystallography (monoclinic, *P2(1)/c* (No. 14), *a* = 14.975 (4) Å, *b* = 18.219 (4) Å, *c* = 20.855 (4) Å, β = 108.20 (2)°, *Z* = 4). A "W" conformation is found for the P–Re–I–Re–P bonds, and a stereoelectronic rationale is given. Models show that if meso bridging halide complex diastereomers were to adopt analogous "W" conformations, severe steric interactions would occur between two syn cyclopentadienyl ligands. Complexes (*RR,SS*)-**4** and (*RR,SS*)-**5** react with acetonitrile (95 °C, 1.25 and 0.25 h, respectively) to give [(η⁵-C₅H₅)Re(NO)(PPh₃)(NCCH₃)]⁺BF$_4^-$ and halide complexes (η⁵-C₅H₅)Re(NO)(PPh₃)(X) (93–99% of theory).

Introduction

The chiral, transition-metal Lewis acid [(η⁵-C₅H₅)Re-(NO)(PPh₃)]⁺ (I) is easily generated in optically active form as a dichloromethane adduct (1), as described in the previous paper and summarized in Scheme I.[1] Lewis acid I binds and activates several types of prochiral organic Lewis bases.[2] These coordinated bases can in many cases be stereospecifically elaborated into chiral organic molecules. However, the binding of *chiral* Lewis bases to I has not yet been systematically examined. With chiral, *racemic* bases, there is the attractive possibility that one enantiomer might be preferentially complexed, affording an optical resolution.

In the previous paper, we reported that optically active dichloromethane complex (*S*)-[(η⁵-C₅H₅)Re(NO)(PPh₃)-(ClCH₂Cl)]⁺BF$_4^-$ ((*S*)-**1**) and optically active chloride

Scheme I. Binding of Optically Active Chloride Complex 2 to the Chiral Lewis Acid [(η⁵-C₅H₅)Re(NO)(PPh₃)]⁺ (I)
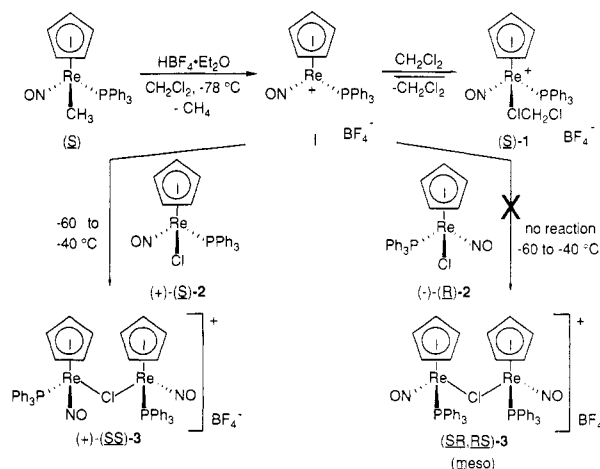
complex (+)-(*S*)-(η⁵-C₅H₅)Re(NO)(PPh₃)(Cl) ((+)-(*S*)-**2**) react at −60 to −40 °C (Scheme I) to give the optically active bridging chloride complex (+)-(*SS*)-[(η⁵-C₅H₅)Re-(NO)(PPh₃)]₂Cl⁺BF$_4^-$ ((+)-(*SS*)-**3**).[1,3] Since both reactants

(1) Fernández, J. M.; Gladysz, J. A. *Organometallics*, preceding paper in this issue.

(2) (a) Fernández, J. M.; Emerson, K.; Larsen, R. D.; Gladysz, J. A. *J. Am. Chem. Soc.* **1986**, *108*, 8268. (b) Fernández, J. M.; Emerson, K.; Larsen, R. D.; Gladysz, J. A. *J. Chem. Soc., Chem. Commun.* **1988**, 37. (c) Bodner, G. S.; Fernández, J. M.; Arif, A. M.; Gladysz, J. A. *J. Am. Chem. Soc.* **1988**, *110*, 4082.

Scheme II. Attempted Synthesis of Bridging Iodide Complex (RR)-4

ON'''Re$^+$'''PPh$_3$, ClCH$_2$Cl (S)-1 + ON'''Re'''PPh$_3$, I (+)-(R)-7 ⇌ ON'''Re'''PPh$_3$, Cl (+)-(S)-2 + ON'''Re$^+$'''PPh$_3$, ICH$_2$Cl (R)-6a

Ph$_3$P'''Re'''NO — X — Re'''PPh$_3$ NO BF$_4^-$
X=Cl, (SS)-3
X= I, (RR)-4
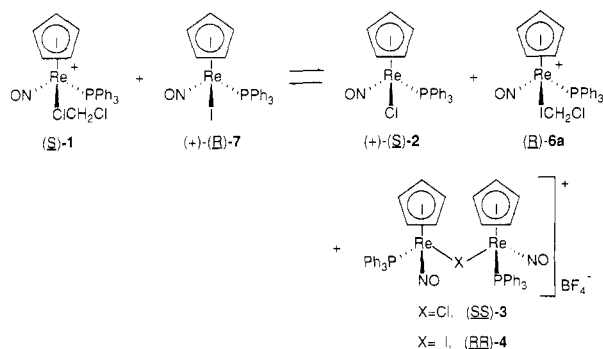
Scheme III. Synthesis and Reactions of Bridging Bromide and Iodide Complexes (RR,SS)-[(η^5-C$_5$H$_5$)Re(NO)(PPh$_3$)]$_2$X$^+$BF$_4^-$

ON'''Re'''PPh$_3$, X
X=I , 7
Br , 8

$\xrightarrow{\text{AgBF}_4}_{\text{C}_6\text{H}_6,\ 80\ °\text{C}}$

Ph$_3$P'''Re'''NO — X — Re'''NO PPh$_3$ BF$_4^-$
X=I , (RR,SS)-4
X=Br, (RR,SS)-5

↓ CH$_3$CN, 80-95 °C

ON'''Re'''PPh$_3$, X + ON'''Re$^+$'''PPh$_3$, NCCH$_3$
9
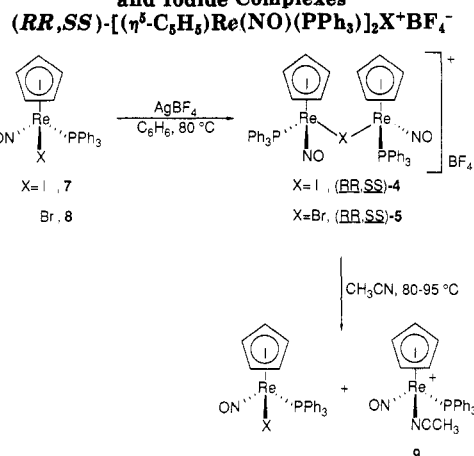
are of the *same* relative configuration, one enantiomer of a *dl* diastereomer is expected. However, when dichloromethane complex (S)-1 and the opposite chloride complex enantiomer (−)-(R)-2 are combined at −60 °C, no reaction occurs. These reactants are of *opposite* relative configurations and should lead to the optically *inactive* meso diastereomer (SR,RS)-3. Upon warming above −40 °C, (S)-1 independently decomposes. No evidence for (SR,-RS)-3 is observed in this and several related reactions. This suggests that the meso diastereomer (SR,RS)-3 is significantly destabilized relative to the *dl* diastereomer. We sought to probe the origin of this stability difference by X-ray crystallography. However, we had difficulty growing suitable crystals of (+)-(SS)-3 or the racemate (±)-(SS,RR)-3.

Hence, we set out to prepare analogous bridging iodide and bromide complexes [(η^5-C$_5$H$_5$)Re(NO)(PPh$_3$)]$_2$I$^+$BF$_4^-$ (4) and [(η^5-C$_5$H$_5$)Re(NO)(PPh$_3$)]$_2$Br$^+$BF$_4^-$ (5) and to determine whether similar *dl*/meso diastereoselectivity occurs. We further sought to acquire an X-ray crystal structure of one of these products and to develop a rationale for the diastereoselection. Finally, we recently reported the synthesis and structural characterization of alkyl iodide complexes of the formula [(η^5-C$_5$H$_5$)Re-(NO)(PPh$_3$)(IR)]$^+$BF$_4^-$ (6).[4] Analysis of the bonding in this scarce but expanding[5] class of complexes should be facilitated by structural comparisons with related iodide and bridging iodide complexes.

Results

I. Synthesis of *dl* Bridging Halide Complexes (RR,SS)-[(η^5-C$_5$H$_5$)Re(NO)(PPh$_3$)]$_2$X$^+$BF$_4^-$. Efforts were first directed at the preparation of optically active bridging iodide complex (RR)-4. Optically active deuteriodichloromethane complex (S)-1-d_2 was generated in CD$_2$Cl$_2$ at −78 °C. Then optically active iodide complex (+)-(R)-(η^5-C$_5$H$_5$)Re(NO)(PPh$_3$)(I) ((+)-(R)-7, 3 equiv),[6] which has the *same* relative configuration, was added (see Scheme II). The reaction was slowly warmed and was

monitored by ^{1}H and ^{31}P NMR. At −60 °C, a complex series of transformations began to occur. Cyclopentadienyl ^{1}H NMR resonances attributable to (RR)-4 (δ 5.39; see racemate isolated below), bridging chloride complex (+)-(SS)-3 (δ 5.36), and three transient species (δ 5.65 and 5.40 and chloride complex (+)-(S)-2 at δ 5.22) slowly appeared. The relative ratios of products and transients changed upon warming, and some ^{1}H NMR chemical shifts varied slightly. The reaction was kept for 2.5 h at room temperature, after which time only (RR)-4 and (+)-(SS)-3 remained ((62 ± 2):(38 ± 2)). These products were inseparable by recrystallization but were further characterized by an IR spectrum. No attempt was made to assay optical purity. However, the products are represented as optically active in Scheme II.

Study of the intermediates in Scheme II revealed a flaw in the synthetic strategy. Analysis by GLC and GLC/MS (of a separate experiment conducted in CH$_2$Cl$_2$) showed the formation of iodochloromethane, ICH$_2$Cl (25%). This suggested a competing *transalkylation* reaction, in which the −CH$_2$Cl moiety of dichloromethane complex (S)-1 undergoes transfer to iodide complex (+)-(R)-7. This would generate chloride complex (+)-(S)-2, which could in turn react with (S)-1 to give bridging chloride complex (+)-(SS)-3 as in Scheme I. In Scheme I, analogous −CH$_2$Cl transfer between reactants would be chemically "invisible".[7]

In accord with this possibility, alkyl halide complexes [(η^5-C$_5$H$_5$)Re(NO)(PPh$_3$)(XR)]$^+$BF$_4^-$ have been shown to be powerful alkylating agents.[4] Hence, an authentic sample of iodochloromethane complex [(η^5-C$_5$H$_5$)Re(NO)-(PPh$_3$)(ICH$_2$Cl)]$^+$BF$_4^-$ (6a) was prepared by the general route reported earlier.[4,8] Its NMR properties matched those of a major (δ 5.65) transient in Scheme II.

Optically active deuteriodichloromethane complex (R)-1-d_2 and optically active iodide complex (+)-(R)-7 (3 equiv), which have *opposite* relative configurations, were also combined at −78 °C and then warmed. Reaction occurred similarly to that of (S)-1 and (+)-(R)-7 (Scheme II), but the relative ratios of intermediates and products differed slightly. The reaction was kept for 2.5 h at room temperature, after which time *dl* bridging halide complexes (RR,SS)-4 and (SS,RR)-3 were present in a (44 ± 2):(56

(3) (a) Absolute configurations are assigned according to the Baird/Sloan modification of the Cahn–Ingold–Prelog priority rules. The η^5-C$_5$H$_5$ ligand is considered to be a pseudoatom of atomic number 30, which gives the following sequence: I > Br > η^5-C$_5$H$_5$ > Cl > PPh$_3$ > NO > CH$_3$. Stanley, K.; Baird, M. C. *J. Am. Chem. Soc.* **1975**, *97*, 6598. Sloan, T. E. *Top. Stereochem.* **1981**, *12*, 1. (b) Prefixes (+) and (−) refer to rotations at 589 nm. (c) The convenient diastereomer descriptor *dl* is rigorously applied only to racemates.

(4) Winter, C. H.; Arif, A. M.; Gladysz, J. A. *J. Am. Chem. Soc.* **1987**, *109*, 7560.

(5) Burk, M. J.; Segmuller, B.; Crabtree, R. H. *Organometallics* **1987**, *6*, 2241.

(6) Merrifield, J. H.; Fernández, J. M.; Buhro, W. E.; Gladysz, J. A. *Inorg. Chem.* **1984**, *23*, 4022.

(7) However, −CH$_2$Cl transfer between (S)-1 and (−)-(R)-2 (but not (+)-(S)-2) leads to racemization.

(8) The isolation (64%) and complete characterization of this compound will be reported in our full paper on alkyl iodide complexes: Winter, C. H.; Veal, W. R.; Garner, C. M.; Arif, A. M.; Gladysz, J. A., submitted for publication.
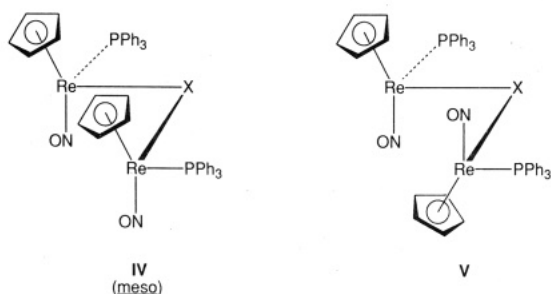
± 2) ratio. In neither this reaction nor Scheme II was evidence for a meso bridging halide complex diastereomer observed.

Other synthetic approaches to bridging halide complexes **4** and **5** were probed. Racemic iodide complex **7** was dissolved in benzene and treated with $AgBF_4$ (Scheme III). The mixture was refluxed, and a product precipitated. Workup gave (*RR,SS*)-**4** in 59% yield. The gross structure of (*RR,SS*)-**4** was evident from its spectroscopic properties and microanalysis (Experimental Section), and the diastereomer assignment was confirmed by an X-ray crystal structure, as described below. A similar reaction of racemic bromide complex $(\eta^5\text{-}C_5H_5)Re(NO)(PPh_3)(Br)$ (**8**) gave bridging bromide complex (*RR,SS*)-**5** in 54% yield. The diastereomer assignment was made by analogy to (*RR,SS*)-**4**. In all cases, only one bridging halide complex diastereomer was evident in the crude and purified reaction mixtures.
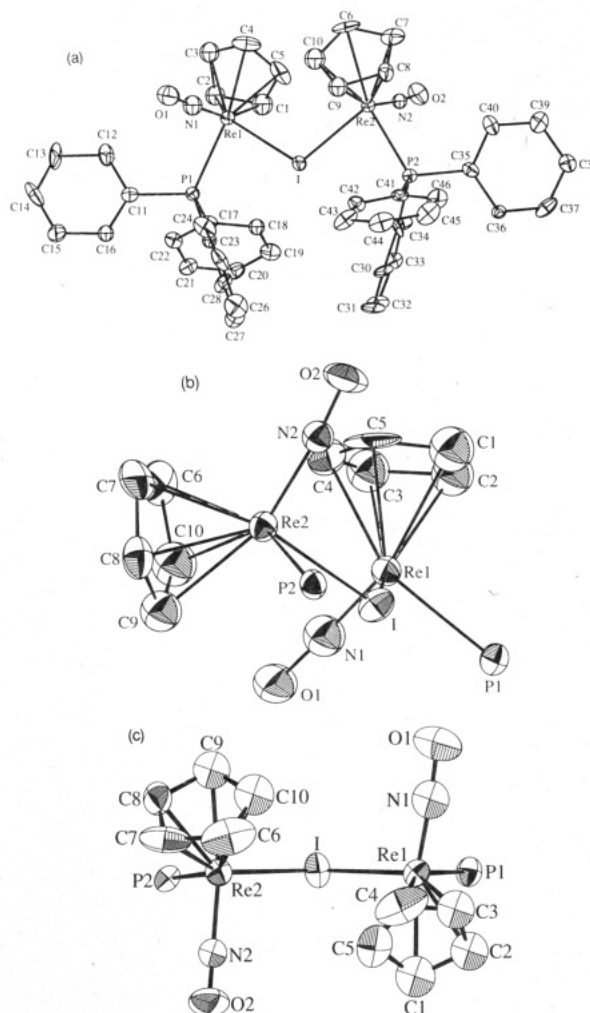
II. Conformation and Crystal Structure of Bridging Iodide Complex (*RR,SS*)-4·$(CHCl_2CHCl_2)_{0.7}$.

We sought to formulate a working conformational hypothesis to account for the greater apparent stability of the *dl* diastereomers of the bridging halide complexes. The alkyl iodide complex $[(\eta^5\text{-}C_5H_5)Re(NO)(PPh_3)(ICH_2Si(CH_3)_3)]^+BF_4^-$ (**6b**) exhibits ca. 90° ON–Re–I, Ph_3P–Re–I, and ON–Re–PPh_3 bond angles in the solid state, as expected from this formally octahedral class of compounds.[4] It also adopts the Re–I conformation shown in Newman projection II, with a P–Re–I–R torsion angle close to 180° (169°).[4] The d orbital HOMO of the chiral Lewis acid fragment I is given in III for comparison.[9]

II
R= $CH_2Si(CH_3)_3$

III
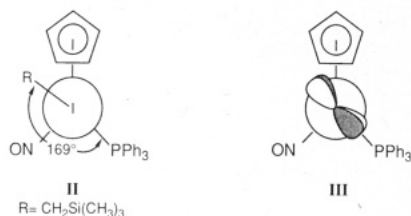
We therefore presumed (as reasoned below) that the meso and *dl* bridging halide complex diastereomers should also prefer to adopt conformations with P–Re–X–Re torsion angles near 180° at *both* rheniums. This restriction enforces a "W" conformation for the P–Re–X–Re–P linkage. The resulting diastereomer structures are shown in IV (meso) and V (*dl*),[3c] with the Re–X–Re bond angles approximated as 90°. There is a severe interaction of two syn cyclopentadienyl ligands in meso diastereomer IV. This is readily verified with molecular models. In contrast, the cyclopentadienyl ligands in diastereomer V are anti, and steric interactions are relieved.

IV
(meso)

V

Recrystallization of (*RR,SS*)-**4** from 1,1,2,2-tetrachloro-

(9) (a) Schilling, B. E. R.; Hoffmann, R.; Faller, J. W. *J. Am. Chem. Soc.* **1979**, *101*, 592. (b) Kiel, W. A.; Lin, G.-Y.; Constable, A. G.; McCormick, F. B.; Strouse, C. E.; Eisenstein, O.; Gladysz, J. A. *Ibid.* **1982**, *104*, 4865.

Figure 1. Structure of the cation of bridging iodide complex (*RR,SS*)-$[(\eta^5\text{-}C_5H_5)Re(NO)(PPh_3)]_2I^+BF_4^-\cdot(CHCl_2CHCl_2)_{0.7}$ ((*RR,SS*)-**4**·$(CHCl_2CHCl_2)_{0.7}$): (a) numbering scheme; (b) view down the I–Re1 bond with phenyl rings omitted; (c) view down the P–Re–I–Re–P "W" with phenyl rings omitted.

ethane/ether gave irregular prisms of (*RR,SS*)-**4**·$(CHCl_2CHCl_2)_{0.7}$. X-ray data were collected under the conditions summarized in Table I. Refinement, described in the Experimental Section, yielded the structure shown in Figure 1. The overall molecular geometry clearly bears a close resemblance to that predicted in V. Bond lengths, bond angles, torsion angles, and positional parameters are summarized in Tables II–V.

III. Reactions of Bridging Halide Complexes.

The reaction of bridging chloride complex (*SS,RR*)-**3** and acetonitrile to give chloride complex **2** and acetonitrile complex $[(\eta^5\text{-}C_5H_5)Re(NO)(PPh_3)(NCCH_3)]^+BF_4^-$ (**9**) was described in the previous paper ($t_{1/2}$ = 60 min, 40.1 °C). Hence, analogous halide bridge cleavages were attempted with (*RR,SS*)-**4** and (*RR,SS*)-**5** (Scheme III). The reaction of (*RR,SS*)-**4** in CD_3CN at 95 °C required 1.25 h to go to completion, as assayed by NMR monitoring. Subsequently isolated from a similar preparative experiment (refluxing CH_3CN) was a (50 ± 2):(50 ± 2) mixture of iodide complex **7** and acetonitrile complex **9** (99%). The reaction of (*RR,SS*)-**5** in CD_3CN at 95 °C required 0.25 h to go to completion. Subsequently isolated from a preparative experiment was a (50 ± 2):(50 ± 2) mixture of bromide complexes **8** and **9** (93%). Thus, the order of bridge stability in bridging halide complexes $[(\eta^5\text{-}C_5H_5)Re(NO)(PPh_3)]_2X^+BF_4^-$ toward cleavage by acetonitrile is I > Br > Cl.

Table I. Summary of Crystallographic Data for
(*RR*,*SS*)-4•(CHCl₂CHCl₂)₀.₇

mol formula	$C_{46}H_{40}BF_4IN_2O_2P_2Re_2 \cdot (C_2H_2Cl_4)_{0.7}$
mol wt	1418.40
cryst system	monoclinic
space group	$P2(1)/c$ (No. 14)
cell dimens (15 °C)	
a, Å	14.975 (4)
b, Å	18.219 (4)
c, Å	20.855 (4)
β, deg	108.20 (2)
V, Å³	5405.2
Z	4
d_{obsd}, g/cm³ (22 °C)	1.752
d_{calcd}, g/cm³ (15 °C)	1.742
cryst dimensions, mm	0.30 × 0.23 × 0.11
diffractometer	Syntex P1̄
radiatn, Å	Mo Kα (0.710 73)
temp of collectn, °C	15 (1)
data collectn method	θ/2θ
scan speed, deg/min	variable, 2.5–8.0
reflctns measured	5947
range/indices	h (0, 17), k (0, 21), l (−24, 24)
scan range	Kα₁ − 1.0 to Kα₂ + 1.0
2θ limit, deg	3.0–41.0
total bkdg time/scan time	0.5
no. of reflctns between std	98
total unique data	5080
obsd data, $I > 3\sigma(I)$	3121
abs coeff, cm⁻¹	53.06
min absorptn correctn	83.72
max absorptn correctn	99.93
no. of variables	503
R(averaging)	0.056, 0.042
Δ/σ(max)	0.03
$R = \sum(||F_o| - |F_c||)/\sum(F_o)$	0.0575
$R_w = \sum(||F_o| - |F_c||)w^{1/2}/ \sum(F_o)w^{1/2}$	0.0620
goodness of fit	3.148
$\Delta\rho$(max), e Å⁻³	1.09, 1.21 Å from Re2

Table II. Bond Lengths in (*RR*,*SS*)-4•(CHCl₂CHCl₂)₀.₇ (Å)

atom 1	atom 2	dist	atom 1	atom 2	dist
Re1	I	2.700 (2)	Re2	I	2.692 (2)
Re1	P1	2.382 (4)	Re2	P2	2.373 (4)
Re1	N1	1.693 (3)	Re2	N2	1.819 (3)
Re1	C1	2.36 (2)	Re2	C6	2.34 (2)
Re1	C2	2.28 (2)	Re2	C7	2.30 (2)
Re1	C3	2.30 (2)	Re2	C8	2.28 (2)
Re1	C4	2.25 (2)	Re2	C9	2.32 (2)
Re1	C5	2.29 (2)	Re2	C10	2.30 (2)
P1	C11	1.81 (2)	P2	C29	1.84 (2)
P1	C17	1.85 (2)	P2	C35	1.79 (2)
P1	C23	1.85 (2)	P2	C41	1.81 (2)
O1	N1	1.27 (1)	O2	N2	1.12 (1)
C1	C2	1.39 (4)	C6	C7	1.49 (3)
C1	C5	1.40 (3)	C6	C10	1.43 (3)
C2	C3	1.50 (4)	C7	C8	1.41 (3)
C3	C4	1.24 (4)	C8	C9	1.43 (3)
C4	C5	1.35 (4)	C9	C10	1.43 (3)
C11	C12	1.41 (2)	C29	C30	1.37 (2)
C11	C16	1.40 (2)	C29	C34	1.40 (2)
C12	C13	1.48 (3)	C30	C31	1.34 (2)
C13	C14	1.36 (3)	C31	C32	1.45 (3)
C14	C15	1.37 (3)	C32	C33	1.36 (2)
C15	C16	1.42 (2)	C33	C34	1.36 (2)
C17	C18	1.43 (2)	C35	C36	1.44 (2)
C17	C22	1.38 (2)	C35	C40	1.40 (2)
C18	C19	1.37 (2)	C36	C37	1.39 (3)
C19	C20	1.48 (3)	C37	C38	1.39 (3)
C20	C21	1.40 (3)	C38	C39	1.42 (3)
C21	C22	1.45 (2)	C39	C40	1.41 (2)
C23	C24	1.41 (2)	C41	C42	1.33 (2)
C23	C28	1.30 (2)	C41	C46	1.45 (2)
C24	C25	1.42 (3)	C42	C43	1.45 (2)
C25	C26	1.41 (3)	C43	C44	1.35 (3)
C26	C27	1.41 (3)	C44	C45	1.42 (3)
C27	C28	1.42 (3)	C45	C46	1.37 (3)
Cl1	C47	1.779	C47	C47	1.392
Cl2	C47	1.777	C48	C49	1.487
Cl3	C48	1.791	F1	B	1.19 (3)
Cl4	C48	1.765	F2	B	1.42 (3)
Cl5	C49	1.715	F3	B	1.31 (3)
Cl6	C49	1.746	F4	B	1.34 (3)

Discussion

Figure 1 shows that bridging iodide complex (*RR*,*SS*)-4 adopts a conformation of approximate C_2 symmetry, with P–Re–I–Re torsion angles (Table IV; 178.8 (2)°, 174.3 (2)°) close to the 180° anticipated in model V above. This places the iodine substituent in the region between the small nitrosyl and medium-sized cyclopentadienyl ligands (Figure 1b), analogously to projection II of related alkyl iodide complex **6b**. There is good experimental and theoretical evidence that this is the sterically least crowded region in which to place a substituent on an atom ligating to Lewis acid I.[10] It is also highly probable, based upon NOE studies with related iron complexes, that this conformational preference of (*RR*,*SS*)-4 is retained in solution.[10a,b]

However, there is also a possible electronic component to this conformational preference. In the previous paper, it was found that Lewis acid I preferentially binds dichloromethane in the presence of appreciable quantities of ether. This contrasts with the solution- and gas-phase binding affinities exhibited by H⁺ and first-row Lewis acids such as BR_3 ($R_3N \gg R_2O \gg RCl$).[11] However, I has the high-lying d-orbital HOMO shown in III, which has no counterpart in first-row Lewis acids. Thus, "Lewis acid" I is more accurately represented as an amphotere, and Lewis base *acceptor* orbitals should play an important role

in determining relative binding affinities to I.

The LUMO of an alkyl halide is generally the C–X σ* orbital.[12] Alkyl halide C–X σ* orbitals are usually lower lying than ether C–O σ* orbitals, as evidenced by the common practice of alkyl halide reduction in etheral solvents. Accordingly, the ca. 180° P–Re–I–C and P–Re–I–Re torsion angles in **6b** and (*RR*,*SS*)-4 maximize overlap of the HOMO of fragment I with C–I and Re–I σ* orbitals. Hence, electronic factors may reinforce the steric conformational considerations noted above. Crabtree has previously emphasized the possibility of d/σ* bonding in alkyl halide and related complexes.[5]

The Re–I–Re bond angle in (*RR*,*SS*)-4 (114.14 (4)°) is larger than the Re–I–C bond angle in alkyl iodide complex **6b** (102.5 (5)°). We presently attribute this to the greater steric demands of the iodine substituents in (*RR*,*SS*)-4. Figure 1c shows that cyclopentadienyl–cyclopentadienyl ligand interactions (compare C4 and C6) are decreased as this angle is increased. Interestingly, the I–Re–N bond angles in (*RR*,*SS*)-4 (98.27 (5)°, 102.78 (5)°) show some of the largest deviations yet observed from idealized octahedral geometry (L–Re–L' = 90°) in this class of compounds.

The Re–I bonds in (*RR*,*SS*)-4 (2.700 (2), 2.692 (2) Å) are slightly longer than that in alkyl iodide complex **6b** (2.678 (1) Å). A probable contributing factor is that the average charge on each rhenium in (*RR*,*SS*)-4 is $+^1/_2$, as opposed

(10) (a) Davies, S. G.; Dordor-Hedgecock, I. M.; Sutton, K. H.; Whittaker, M. W. *J. Am. Chem. Soc.* **1987**, *109*, 5711. (b) Hunter, B. K.; Baird, M. C. *Organometallics* **1985**, *4*, 1481. (c) Georgiou, S.; Gladysz, J. A. *Tetrahedron* **1986**, *42*, 1109.

(11) (a) Long, J.; Munson, B. *J. Am. Chem. Soc.* **1973**, *95*, 2427. (b) West, R.; Powell, D. L.; Whatley, L. S.; Lee, M. K. T.; Schleyer, P. v. R. *Ibid.* **1962**, *84*, 3221. (c) Drago, R. S.; Wayland, B. B. *Ibid.* **1965**, *87*, 3571. (d) Coyle, T. D.; Stone, F. G. A. *Prog. Boron Chem.* **1964**, *1*, 83.

(12) Oritz, J. V.; Havlas, Z.; Hoffmann, R. *Helv. Chim. Acta* **1984**, *67*, 1.

Table III. Bond Angles in (RR,SS)-4·$(CHCl_2CHCl_2)_{0.7}$ (deg)

atom 1	atom 2	atom 3	angle	atom 1	atom 2	atom 3	angle
I	Re1	P1	87.4 (1)	I	Re2	P2	86.6 (1)
I	Re1	N1	102.78 (5)	I	Re2	N2	98.27 (5)
P1	Re1	N1	92.4 (1)	P2	Re2	N2	90.4 (1)
Re1	N1	O1	176.6 (8)	Re2	N2	O2	173.1 (8)
Re1	I	Re2	114.14 (4)	Re2	P2	C29	116.1 (6)
Re1	P1	C11	115.4 (5)	Re2	P2	C35	113.5 (6)
Re1	P1	C17	114.3 (6)	Re2	P2	C41	113.0 (6)
Re1	P1	C23	116.1 (5)	C29	P2	C35	101.8 (8)
C11	P1	C17	104.4 (8)	C29	P2	C41	105.2 (7)
C11	P1	C23	104.2 (8)	C35	P2	C41	106.1 (9)
C17	P1	C23	100.6 (8)	P2	C29	C30	123 (1)
P1	C11	C12	118 (1)	P2	C29	C34	118 (1)
P1	C11	C16	121 (1)	P2	C35	C36	119 (1)
P1	C17	C18	116 (1)	P2	C35	C40	121 (1)
P1	C17	C22	119 (1)	P2	C41	C42	119 (1)
P1	C23	C24	115 (2)	P2	C41	C46	122 (1)
P1	C23	C28	125 (1)	C7	C6	C10	105 (2)
C2	C1	C5	106 (2)	C6	C7	C8	106 (2)
C1	C2	C3	104 (2)	C8	C9	C10	105 (2)
C1	C5	C4	110 (2)	C6	C10	C9	112 (2)
C2	C3	C4	110 (3)	C7	C8	C9	112 (2)
C3	C4	C5	110 (3)	C30	C31	C32	121 (2)
C13	C14	C15	125 (2)	C30	C29	C34	119 (2)
C12	C11	C16	121 (2)	C31	C32	C33	118 (2)
C11	C12	C13	120 (2)	C29	C30	C31	120 (2)
C14	C15	C16	120 (2)	C36	C35	C40	120 (2)
C11	C16	C15	118 (2)	C32	C33	C34	120 (2)
C12	C13	C14	115 (2)	C35	C36	C37	120 (2)
C19	C20	C21	119 (2)	C29	C34	C33	122 (2)
C18	C17	C22	124 (2)	C36	C37	C38	122 (2)
C17	C18	C19	119 (2)	C37	C38	C39	118 (2)
C20	C21	C22	121 (2)	C42	C41	C46	118 (2)
C17	C22	C21	117 (2)	C38	C39	C40	122 (2)
C18	C19	C20	119 (2)	C41	C42	C43	123 (2)
C24	C25	C26	121 (2)	C35	C40	C39	118 (2)
C24	C23	C28	121 (2)	C42	C43	C44	116 (2)
C25	C26	C27	115 (2)	C41	C46	C45	120 (2)
C23	C24	C25	119 (2)	C43	C44	C45	123 (2)
C26	C27	C28	123 (2)	C44	C45	C46	119 (2)
C23	C28	C27	120 (2)	Cl1	C47	Cl2	106.8
Cl1	C47	C47	112.2	Cl2	C47	C47	111.9
Cl3	C48	Cl4	107.7	F1	B	F2	108 (2)
Cl5	C49	Cl6	97.8	F1	B	F3	116 (3)
Cl3	C48	C49	120.6	F1	B	F4	114 (3)
Cl4	C48	C49	108.3	F2	B	F3	112 (2)
Cl5	C49	C48	104.7	F2	B	F4	99 (2)
Cl6	C49	C48	111.4	F3	B	F4	107 (2)

Table IV. Selected Torsion Angles (deg) in (RR,SS)-4·$(CHCl_2CHCl_2)_{0.7}$

atom 1	atom 2	atom 3	atom 4	angle
P1	Re1	I	Re2	178.8 (2)
P2	Re2	I	Re1	174.3 (2)
N1	Re1	I	Re2	89.4 (9)
N2	Re2	I	Re1	84.4 (9)

to +1 in **6b**. We predict that the crystal structure of iodide complex $(\eta^5\text{-}C_5H_5)Re(NO)(PPh_3)(I)$ will show a still longer Re–I bond, due to increased Re/I lone pair repulsion and the absence of any attractive d/σ^* interaction. A similar lengthening trend is observed in phosphido complex $(\eta^5\text{-}C_5H_5)Re(NO)(PPh_3)(PPh_2)$ with the Re–PPh_3 and Re–PPh_2 bonds.[13]

The structures of several related bridging halide complexes have been reported.[14] Iron complex $[(\eta^5\text{-}C_5H_5)\text{-}Fe(CO)_2]_2I^+BF_4^-$ exhibits a smaller M–I–M bond angle

(13) Buhro, W. E.; Zwick, B. D.; Georgiou, S.; Hutchinson, J. P.; Gladysz, J. A. *J. Am. Chem. Soc.* **1988**, *110*, 2427.

(14) (a) Cotton, F. A.; Frenz, B. A.; White, A. J. *J. Organomet. Chem.* **1973**, *60*, 147. (b) Cupertino, D. C.; Harding, M. M.; Cole-Hamilton, D. J.; Dawes, H. M.; Hursthouse, M. B. *J. Chem. Soc., Dalton Trans.* **1986**, 1129.

(110.8 (1)°) than (RR,SS)-4, consistent with the lesser steric requirements on the iron ligands.[14a] This complex lacks the steric and electronic features that promote a "W" conformation in (RR,SS)-4, and hence the Fe–I–Fe bonds twist to place the cyclopentadienyl ligands much further apart.

In summary, this study has shown that the chiral Lewis acid **I** exhibits an extraordinary selectivity for binding one enantiomer of rhenium halide complexes $(\eta^5\text{-}C_5H_5)Re$-$(NO)(PPh_3)(X)$. This selectivity is rationalized by a simple conformational model, which has a corollary of potentially practical impact. Note that in bridging halide complex diastereomers **IV** and **V**, the large ligand on each rhenium (PPh_3) is anti to the Re–I bond of the *opposite* rhenium. However, only in the preferred diastereomer **V** is the medium-sized ligand on each rhenium (C_5H_5) syn to the small ligand (NO) on the opposite rhenium. Consider next the generalized case of a carbon-substituted Lewis base :XCLMS with three sterically differentiated ligands on carbon (L, M, S). Two diastereomeric adducts with Lewis acid **I** are possible (**VI**, **VII**). Analogous reasoning indicates that **VII**, in which the medium-sized carbon substituent (M) is syn to the small ligand on rhenium (NO), should be the more stable. Hence, this excercise in inorganic conformational analysis leads to the prediction that one enantiomer of Lewis bases such as methyl-substituted secondary alkoxides $R(CH_3)CHO^-$ and methyl-substituted secondary alkyl iodides $R(CH_3)CHI$ should preferentially bind to chiral Lewis acid **I**.

VI　　　　　　　　　　　　　　　　　VII
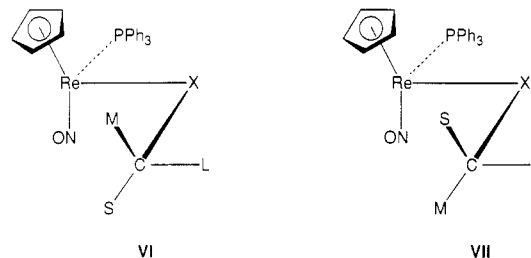
Experimental Section

General Data. Reaction procedures and instrumentation utilized were as described in the previous paper.[1] All GLC analyses were conducted on a Hewlett-Packard 5890A gas chromatograph equipped with a FID detector. Microanalyses were conducted by Schwarzkopf Laboratories. Melting points were determined in evacuated capillaries and were not corrected. Reagents AgBF₄, ICH₂Cl, and n-decane were used as received from Aldrich. Solvent 1,1,2,2-tetrachloroethane was distilled from P_2O_5. Other solvents were purified and HBF_4·$O(C_2H_5)_2$ was standardized as described in the previous paper.[1]

Preparation of (RR,SS)-[$(\eta^5\text{-}C_5H_5)Re(NO)(PPh_3)]_2I^+BF_4^-$ ((RR,SS)-4). A Schlenk flask was charged with $(\eta^5\text{-}C_5H_5)Re$-$(NO)(PPh_3)(I)$ (7, 0.249 g, 0.371 mmol),[6] AgBF₄ (0.086 g, 0.444 mmol), benzene (20 mL), and a stir bar and was fitted with a reflux condenser. The reaction was refluxed with stirring for 0.5 h, and the volatiles were then removed in vacuo. The residue was extracted with CH_2Cl_2 (25 mL), and the extract was filtered through a 2-cm Celite pad. Ether (100 mL) was added to the filtrate, and a light orange powder precipitated. The powder was collected by filtration and precipitated two additional times from CH_2Cl_2/ether. The light orange powder was then dried under vacuum to give analytically pure (RR,SS)-4 (0.141 g, 0.108 mmol, 59%): mp 253–256 °C dec; IR (cm^{-1}, KBr) ν_{NO} 1675 (s); ^{1}H NMR (δ, CD_2Cl_2) 7.50–7.24 (m, PPh_3), 5.40 (s, C_5H_5); ^{13}C NMR (ppm, CD_2Cl_2) PPh_3 at 134.10 (d, $J = 56.1$ Hz, *ipso*), 133.77 (d, $J = 10.6$ Hz), 131.57 (d, $J = 2.7$ Hz, para), 129.14 (d, $J = 11.0$ Hz), 92.09 (s, C_5H_5); ^{31}P NMR (ppm, CD_2Cl_2) 12.1 (s). Anal. Calcd for $C_{46}H_{40}BF_4IN_2O_2P_2Re_2$: C, 42.47; H, 3.10. Found: C, 42.06; H, 3.26.

Preparation of (RR,SS)-[$(\eta^5\text{-}C_5H_5)Re(NO)(PPh_3)]_2Br^+$-$BF_4^-$ ((RR,SS)-5). A Schlenk flask was charged with (η^5-

Table V. Positional Parameters for (*RR*,*SS*)-4•(CHCl₂CHCl₂)₀.₇[a,b]

atom	x	y	z	B, Å²	atom	x	y	z	B, Å²
Re1	0.25436 (8)	0.02180 (5)	0.39360 (6)	3.05 (2)	C27	0.330 (2)	−0.289 (2)	0.445 (2)	7 (1)
Re2	0.25274 (8)	0.03323 (5)	0.61001 (5)	2.89 (2)	C28	0.280 (2)	−0.234 (2)	0.399 (2)	5.3 (8)
I	0.2595 (2)	−0.05270 (9)	0.5066 (1)	3.74 (4)	C29	0.186 (2)	−0.155 (1)	0.616 (1)	3.0 (6)
P1	0.2596 (5)	−0.0939 (4)	0.3417 (3)	3.1 (2)	C30	0.228 (2)	−0.222 (1)	0.617 (1)	4.0 (7)
P2	0.2443 (5)	−0.0770 (4)	0.6685 (3)	2.8 (2)	C31	0.183 (2)	−0.276 (1)	0.576 (2)	6 (1)
O1	0.457 (1)	0.051 (1)	0.416 (1)	7.1 (7)	C32	0.089 (2)	−0.265 (2)	0.530 (1)	4.8 (8)
O2	0.049 (1)	0.057 (1)	0.572 (1)	5.9 (6)	C33	0.046 (2)	−0.199 (1)	0.532 (1)	3.9 (7)
N1	0.3694	0.0382	0.4045	5*	C34	0.095 (2)	−0.144 (1)	0.572 (1)	4.4 (8)
N2	0.1257	0.0436	0.5866	3*	C35	0.178 (2)	−0.068 (1)	0.726 (1)	3.8 (7)
C1	0.0916	0.0472	0.3559	6*	C36	0.148 (2)	−0.133 (1)	0.753 (1)	2.9 (6)
C2	0.132 (3)	0.062 (2)	0.306 (2)	10 (1)	C37	0.099 (2)	−0.127 (2)	0.799 (2)	5.6 (8)
C3	0.195 (3)	0.126 (2)	0.333 (2)	10 (1)	C38	0.077 (2)	−0.059 (2)	0.820 (1)	4.2 (7)
C4	0.200 (3)	0.137 (2)	0.393 (2)	7 (1)	C39	0.107 (2)	0.005 (2)	0.793 (1)	5.8 (8)
C5	0.138 (2)	0.093 (2)	0.410 (2)	6.8 (9)	C40	0.157 (2)	0.001 (2)	0.746 (1)	4.1 (7)
C6	0.306 (2)	0.154 (2)	0.607 (2)	7 (1)	C41	0.359 (2)	−0.111 (1)	0.718 (1)	4.0 (7)
C7	0.301 (2)	0.136 (2)	0.676 (2)	6 (1)	C42	0.423 (2)	−0.125 (1)	0.687 (1)	3.9 (7)
C8	0.366 (2)	0.079 (2)	0.701 (1)	4.6 (8)	C43	0.516 (2)	−0.153 (2)	0.722 (2)	5.9 (9)
C9	0.412 (2)	0.057 (2)	0.654 (2)	5.7 (8)	C44	0.538 (2)	−0.160 (2)	0.790 (2)	6 (1)
C10	0.374 (3)	0.103 (2)	0.596 (2)	6.7 (9)	C45	0.473 (2)	−0.145 (2)	0.826 (2)	7 (1)
C11	0.318 (2)	−0.094 (1)	0.278 (1)	3.4 (7)	C46	0.386 (2)	−0.120 (2)	0.791 (1)	5.2 (8)
C12	0.310 (2)	−0.031 (2)	0.237 (1)	5.2 (8)	C47	0.0428	−0.5010	0.5257	4*
C13	0.350 (2)	−0.031 (2)	0.180 (1)	7 (1)	C48	0.2712	−0.6280	0.4739	6*
C14	0.401 (2)	−0.092 (2)	0.177 (2)	7.8 (9)	C49	0.2910	0.0683	0.9316	6*
C15	0.409 (2)	−0.154 (2)	0.215 (2)	5.7 (9)	Cl1	0.1378 (7)	−0.0286 (5)	0.9979 (5)	4.8 (2)
C16	0.370 (2)	−0.155 (2)	0.269 (1)	3.9 (7)	Cl2	−0.0425	−0.5563	0.4054	5*
C17	0.143 (2)	−0.135 (1)	0.299 (1)	3.8 (7)	Cl3	0.3588	−0.6955	0.5118	3*
C18	0.081 (2)	−0.142 (1)	0.339 (1)	3.8 (6)	Cl4	0.1691	−0.6749	0.4258	5*
C19	−0.003 (2)	−0.177 (2)	0.313 (2)	5.1 (9)	Cl5	0.3815	0.0194	0.9856	3*
C20	−0.031 (2)	−0.204 (2)	0.242 (2)	5.0 (8)	Cl6	0.3515	−0.6014	0.3783	5*
C21	0.033 (2)	−0.197 (2)	0.206 (1)	4.7 (8)	B	0.165 (3)	−0.670 (2)	0.633 (2)	5.1 (8)
C22	0.122 (2)	−0.159 (1)	0.234 (1)	3.8 (7)	F1	0.218 (2)	−0.628 (2)	0.621 (2)	14 (1)
C23	0.317 (2)	−0.170 (1)	0.399 (1)	3.3 (6)	F2	0.212 (2)	−0.705 (2)	0.695 (1)	10.0 (9)
C24	0.407 (2)	−0.153 (2)	0.443 (2)	6.0 (9)	F3	0.083 (2)	−0.642 (2)	0.632 (1)	9.7 (8)
C25	0.454 (2)	−0.205 (2)	0.493 (1)	5.6 (8)	F4	0.147 (3)	−0.730 (2)	0.593 (2)	13 (1)
C26	0.416 (3)	−0.276 (2)	0.495 (2)	8 (1)					

[a] Atoms with an asterisk were refined isotropically. [b] Atoms refined anisotropically are given in the form of the isotropic equivalent displacement parameter, defined as $(^4/_3)[a^2B(1,1) + b^2B(2,2) + c^2B(3,3) + ab(\cos \gamma)B(1,2) + ac(\cos \beta)B(1,3) + bc(\cos \alpha)B(2,3)]$.

$C_5H_5Re(NO)(PPh_3)(Br)$ (8, 0.121 g, 0.194 mmol),[6] $AgBF_4$ (0.054 g, 0.277 mmol), benzene (10 mL), and a stir bar and was fitted with a reflux condenser. The reaction was refluxed with stirring for 0.5 h, and the volatiles were then removed in vacuo. The residue was extracted with CH_2Cl_2 (25 mL), and the extract was filtered through a 2-cm Celite pad. Ether (100 mL) was added to the filtrate, and a tan powder precipitated. The precipitate was dissolved in CH_2Cl_2, and ether was added by vapor diffusion. Fine orange feathers formed. These were collected by filtration, recrystallized, and dried under vacuum to give (*RR*,*SS*)-5 (0.066 g, 0.053 mmol, 54%): mp 244–248 °C dec; IR (cm⁻¹, KBr) ν_{NO} 1664 (s); ¹H NMR (δ, CD_2Cl_2) 7.55–7.17 (m, PPh₃), 5.38 (s, C_5H_5); ¹³C NMR (ppm, CD_2Cl_2) PPh₃ at 133.84 (d, J = 10.7 Hz), 133.48 (d, J = 55.9 Hz, ipso), 131.66 (d, J = 2.2 Hz, para), 129.24 (d, J = 10.9 Hz), 92.78 (s, C_5H_5); ³¹P NMR (ppm, CD_2Cl_2) 12.8 (s). Anal. Calcd for $C_{46}H_{40}BBrF_4N_2O_2P_2Re_2$: C, 44.06; H, 3.22. Found: C, 44.19; H, 3.49.

Reactions of [(η⁵-C₅H₅)Re(NO)(PPh₃)(ClCH₂Cl)]⁺BF₄⁻ (1) and 1-*d*₂ with (η⁵-C₅H₅)Re(NO)(PPh₃)(I) (7). A. A 5-mm NMR tube was charged with (+)-(S)-(η⁵-C₅H₅)Re(NO)(PPh₃)-(CH₃) (0.031 g, 0.056 mmol)[15] and CD_2Cl_2 (0.70 mL) and capped with a septum. The tube was cooled to −78 °C, and HBF₄·Et₂O (0.0075 mL, 0.059 mmol) was added to give (S)-1-*d*₂. Then (+)-(R)-7 (0.111 g, 0.165 mmol)[6] was added, and the tube was transferred to a −80 °C NMR probe. The probe was slowly warmed to 20 °C, and ¹H NMR spectra were recorded at 10 °C intervals. After 2.5 h at 20 °C, the reaction was complete by ¹H NMR ((*RR*)-4, δ 5.40, 68%; (+)-(SS)-3, δ 5.39, 32%). **B.** A 5-mm NMR tube was charged with (−)-(R)-(η⁵-C₅H₅)Re(NO)(PPh₃)(CH₃) (0.026 g, 0.046 mmol)[15] and CD_2Cl_2 (0.70 mL) and was fitted with a septum. The tube was cooled to −78 °C, and HBF₄·Et₂O (0.0064 mL, 0.050 mmol) was added to give (R)-1-*d*₂. Then (+)-(R)-7 (0.094

g, 0.140 mmol) was added. The reaction was monitored as in experiment A; see text for data. **C.** A Schlenk flask was charged with (η⁵-C₅H₅)Re(NO)(PPh₃)(CH₃) (0.065 g, 0.117 mmol), CH_2Cl_2 (2 mL), and a stir bar and was fitted with a rubber septum. The solution was cooled to −78 °C and stirred. Then HBF₄·Et₂O (0.0165 mL, 0.130 mmol) was added, followed by 7 (0.244 g, 0.364 mmol). The reaction was slowly warmed and stirred at room temperature for 3.5 h. Then *n*-decane (0.023 mL, 0.118 mmol) was added. Analysis by GLC (25 m, 5% phenyl methyl silicone glass capillary column) and GLC/MS indicated a 25% yield of ICH_2Cl versus *n*-decane.

Reactions of (*RR*,*SS*)-4 and (*RR*,*SS*)-5 with CH₃CN. A. A Schlenk flask was charged with (*RR*,*SS*)-4 (0.0283 g, 0.0218 mmol), CH₃CN (5 mL), and a stir bar. The orange solution was refluxed with stirring for 5 h. The solvent was removed in vacuo, and the orange-red residue was vacuum dried (0.1 mm, 6 h) to afford 0.0291 g of an orange powder. Analysis by ¹H and ³¹P NMR showed 7 and [(η⁵-C₅H₅)Re(NO)(PPh₃)(NCCH₃)]⁺BF₄⁻ (9)[1] to be the only products. Integration of the cyclopentadienyl resonances indicated a (50 ± 2):(50 ± 2) 7/9 ratio (0.0216 mmol, 99% each). **B.** A 5-mm NMR tube was charged with (*RR*,*SS*)-4 (0.191 g, 0.147 mmol) and CD₃CN (0.7 mL), capped with a septum, and placed in a 95 °C bath. Data: see text. **C.** Experiments identical with the preceding were carried out with (*RR*,*SS*)-5 on 0.0176- and 0.0143-mmol scales, respectively. Data: see text.

X-ray Crystal Structure of (*RR*,*SS*)-4·(CHCl₂CHCl₂)₀.₇. A sample of (*RR*,*SS*)-4 was recrystallized from 1,1,2,2-tetra-chloroethane/ether. This gave (*RR*,*SS*)-4·(CHCl₂CHCl₂)₀.₇ as irregular deep orange prisms, mp 247–250 °C dec. Anal. Calcd for $C_{46}H_{40}BF_4IN_2O_2P_2Re_2$·(C₂H₂Cl₄)₀.₇: C, 40.14; H, 2.94; Cl, 7.00. Found: C, 40.09; H, 2.84; Cl, 7.21. ¹H NMR (δ, CD_2Cl_2): 6.03 (0.7 H vs C₅H₅).

An orange prism of (*RR*,*SS*)-4·(CHCl₂CHCl₂)₀.₇ was mounted on a glass fiber, and data were collected as described in Table I. Cell constants and an orientation matrix for data collection were obtained from least-squares refinement, using the setting

(15) Merrifield, J. H.; Strouse, C. E.; Gladysz, J. A. *Organometallics* **1982**, *1*, 1204.

angles of 15 reflections in the range 18° < 2θ < 24°. The space group was determined from the systematic absences (h01, l = 2n; 0k0, k = 2n) and subsequent least-squares refinement.

A total of 5947 reflections were collected. As a check on crystal and electronic stability, two representative reflections were measured every 98 reflections. The intensities of these standards remained constant within experimental error throughout data collection. No decay correction was applied.

Lorentz and polarization corrections, and an empirical absorption correction based upon a series of ψ scans, were applied to the data. Intensities of equivalent reflections were averaged, and two reflections were rejected because their intensities differed significantly from the average. The agreement factors for the averaging of the 284 observed and accepted reflections was 5.6% based upon intensity and 4.2% based upon F_o.

The structure was solved by the Patterson heavy-atom method. The structure was refined in full-matrix least squares where the function minimized was $\Sigma w(|F_o| - |F_c|)^2$, with a weight w of 1.0 for all observed reflections. All non-hydrogen atoms, except N1, N2, C1, B, and all but C11 in the $CHCl_2CHCl_2$ molecules, were refined with anisotropic thermal parameters. One $CHCl_2CHCl_2$ molecule (that containing C47) was situated on a crystallographic inversion center with full occupancy $((RR,SS)$-4·$/CHCl_2CHCl_2$ = 1.0/0.5). A second $CHCl_2CHCl_2$ molecule was also found and was assigned an occupancy of 0.2, in accord with the analytical data; this gave satisfactory refinement and reasonable thermal parameters. Scattering factors, and $\Delta f'$ and $\Delta f''$ values, were taken

from the literature.[16] Anomalous dispersion effects were included in F_c.[17] The final refinement cycle converged to R and R_w values given in Table I. The highest peak in the final difference Fourier had a height of 1.09 e Å^{-3}, with an estimated error based upon Δf of 0.20.[18] All calculations were performed on a VAX 8300 computer with the SDP/VAX package.[19]

Supplementary Material Available: A table of anisotropic thermal parameters for (RR,SS)-4·$(CHCl_2CHCl_2)_{0.7}$ (2 pages); a listing of calculated and observed structure factors for (RR,SS)-4·$(CHCl_2CHCl_2)_{0.7}$ (11 pages). Ordering information is given on any current masthead page.

(16) Cromer, D. T.; Waber, J. T. in *International Tables for X-ray Crystallography*; Ibers, J. A., Hamilton, W. C., Eds.; Kynoch: Birmingham, England, 1974; Volume IV, Tables 2.2B and 2.3.1.
(17) Ibers, J. A.; Hamilton, W. C. *Acta Crystallogr.* 1964, *17*, 781.
(18) Cruickshank, D. W. J. *Acta Crystallogr.* 1949, *2*, 154.
(19) Frenz, B. A. The Enraf-Nonius CAD 4 SDP—A Real-time System for Concurrent X-ray Data Collection and Crystal Structure Determination. In *Computing and Crystallography*; Schenk, H., Olthof-Hazelkamp, R., van Konigsveld, H., Bassi, G. C., Eds.; Delft University Press: Delft, Holland, 1978; pp 64–71.

Biomimetic Organometallic Chemistry: Regio- and Stereoselectivity in the Hydroxylation Reaction of Cyclohexyltriphenyltin with Metalloporphyrins as the Biomimetic Catalysts and Iodosylbenzene as the Oxygen Transfer Agent

Richard H. Fish* and Robert T. Price

Lawrence Berkeley Laboratory, University of California, Berkeley, California 94720

Received May 18, 1988

The regio- and stereoselectivity in the hydroxylation reaction of cyclohexyltriphenyltin (1), with biomimetic catalysts that mimic the active site of cytochrome P-450 monooxygenase enzyme, iron(III), and manganese(III) tetrakis(pentafluorophenyl)porphyrin derivatives [Fe^{III} or $Mn^{III}TF_5PP(Br,OAc)$], was studied with the oxygen transfer agent, iodosylbenzene, and the results were compared to those results previously obtained with the P-450 enzyme from rat liver microsomes. The $Mn^{III}TF_5PP(OAc)$ biomimetic catalyst provided a 22% conversion of 1 to a mixture of *cis*- and *trans*-hydroxycyclohexyltriphenyltin compounds that included the trans-4 (5.9%), 2; cis-3 (22%), 3; trans-3 (3.3%), 4; and trans-2 (68.8%), 5, isomers. The regiochemistry on a per hydrogen basis shows a C4:C3:C2:C1 ratio of 1:2:6:0 and a high stereoselectivity for equatorial over axial hydroxyl products with a EQ/AX ratio of 29. The corresponding $Fe^{III}TF_5PP(Br)$ catalyst gave the same pattern of hydroxylation as with the above-mentioned Mn catalyst. In comparison to the P-450 enzyme, which had a different regioselectivity ratio on a per hydrogen basis for C4:C3:C2:C1 of 109:7:1:0, the biomimics appear to have less steric requirements at the active site. Mechanistically the tin atom also appears to control the regiochemistry of the hydroxylation reaction by the fact that 3 and 5 are the major hydroxylation products due to a stabilization of radical intermediates on carbons 2 and 3 by the tin–carbon σ bond. As well, the hydroxyl rebound reaction to give products 2–5 also appears to be stereoselective for the sterically more favorable equatorial product.

Introduction

The recent interest in the synthesis of biomimetic catalysts that mimic the biologically important cytochrome P-450 dependent monooxygenase enzyme reaction[1] by converting C–H bonds to C–OH bonds in a regio- and

stereoselective manner has led to an enormous number of contributions that have clearly shown similar reactivity to the reactive metal center of that enzyme.[2] While the types

(1) (a) Ullrich, V. *Angew. Chem., Int. Ed. Engl.* 1972, *11*, 701 and references therein. (b) *Molecular Mechanism of Oxygen Activation*; Hayaishi, O., Ed.; Academic: New York, 1974. (c) Guengerich, F. P.; MacDonald, T. L. *Acc. Chem. Res.* 1984, *17*, 9. (d) White, R. E.; Coon, M. J.; *Annu. Rev. Biochem.* 1980, *49*, 315. (e) Coon, M. J.; White, R. E. In *Dioxygen Binding and Activation by Metal Centers*; Spiro, T. G., Ed.; Wiley: New York, 1980; p 73.

(2) (a) Groves, J. T.; Nemo, T. E.; Myers, R. S. *J. Am. Chem. Soc.* 1979, *101*, 1032. (b) Chang, C. K.; Ebina, F. *J. Chem. Soc., Chem. Commun.* 1981, 778. (c) Hill, C. L.; Schardt, B. C. *J. Am. Chem. Soc.* 1980, *102*, 6375. (d) Groves, J. T.; Nemo, T. E. *J. Am. Chem. Soc.* 1983, *105*, 6243. (e) Fontecave, M.; Mansuy, D. *Tetrahedron* 1984, *21*, 4297. (f) Suslick, K.; Cook, B., Fox, M. *J. Chem. Soc., Chem. Commun.* 1985, 580. (g) Smegal, J. A.; Shardt, B. C.; Hill, C. L. *J. Am. Chem. Soc.* 1983, *105*, 3510. (h) DePoorter, B.; Ricci, M.; Meunier, G. *Tetrahedron Lett.* 1985, *26*, 4459. (i) Nappa, M. J.; Tolman, C. A. *Inorg. Chem.* 1985, *24*, 4711. (j) Cook, B. R.; Reinert, T. J.; Suslick, K. S. *J. Am. Chem. Soc.* 1986, *108*, 7281. (k) Smegal, J.; Hill, C. L. *J. Am. Chem. Soc.* 1983, *105*, 3515.